DOI:
10.1002/dvdy.24401

Document Version
Peer reviewed version

ECM couples the convergence movements of mesoderm and neural plate during the early stages of neurulation

Claudio Araya[1,2 *]
Email: claudio.araya@uach.cl

Carlos Carmona-Fontaine[3]
Email: carmonac@mskcc.org

Jonathan DW Clarke[1*]
Email: jon.clarke@kcl.ac.uk

[*]Corresponding authors

1. CA's current address:
Laboratory of Developmental Biology
Instituto de Ciencias Marinas y Limnológicas
Facultad de Ciencias
Universidad Austral de Chile
Campus Isla Teja s/n
Valdivia, 5090000
Chile

2. C C-F's current address:
Program in Computational Biology,
Memorial Sloan-Kettering Cancer Center,
New York, NY 10065, USA.

3. JDWC's current address:
MRC Centre for Developmental Neurobiology
King's College London
New Hunt's House, 4th Floor
Guy's Hospital Campus
London SE1 1UL

ABSTRACT

Background: During the initial stages zebrafish neurulation, neural plate cells undergo highly coordinated movements before they assemble into a multi-cellular solid neural rod. We have previously identified that the underlying mesoderm is critical to ensure such coordination and generate correct neural tube organization. However, how inter-tissue co-ordination is achieved *in vivo* during zebrafish neural tube morphogenesis is unknown.

Results: In this work, we use quantitative live imaging to study the co-ordinated movements of neural ectoderm and mesoderm during dorsal tissue convergence. We show the extracellular matrix components Laminin and Fibronectin that lie between mesoderm and neural plate act to couple the movements of neural plate and mesoderm during early stages of neurulation and to maintain the close apposition of these two tissues.

Conclusions: Our study highlights the importance of the ECM proteins Laminin and Fibronectin in coupling the movements and spatial proximity of mesoderm and neuroectoderm during the morphogenetic movements of neurulation.

Running title: ECM is required during zebrafish neurulation

Keywords

Zebrafish; neurulation; morphogenesis; extracellular matrix

Highlights

1. Laminin and Fibronectin are required during early zebrafish neurulation.
2. Laminin and Fibronectin maintain the normal close apposition of mesoderm and neural plate.
3. Laminin and Fibronectin couple convergence movements between neural plate and mesoderm.

INTRODUCTION

Neural tube formation in zebrafish embryos is a complex process that initially involves the coordinated movements of neural progenitor cells towards the dorsal midline and the subsequent generation of a well-organized apico-basal polarity at the midline seam (Ciruna et al., 2006; Hong and Brewster, 2006; Tawk et al., 2007; Zigman et al., 2011). In recent years, others, and we have shown that the establishment of this cell polarity is controlled by a series of cell behaviours, including mid-line cell division and contra-lateral cell-cell interaction at the nascent midline at rod stages (Tawk et al., 2007; Quesada-Hernandez et al., 2010; Zigman et al., 2011; Buckley et al., 2013). Because neural polarisation appears to be regulated by a timing mechanism rather than the exact environment of the dorsal midline (Girdler et al., 2013), the efficient convergence movement of neural plate cells towards the dorsal midline are critical to ensure neural cells are in the right place to initiate apicobasal polarisation (Hong and Brewster, 2006; Tawk et al., 2007). Additionally we have shown that interactions with adjacent tissues like the underlying mesoderm are necessary for co-ordinated movements of the neural plate cells (Araya et al., 2014). In fact, our previous analysis indicates that the movements between the neuroectoderm and the underlying mesoderm are highly coupled during initial stages of zebrafish neurulation (Araya et al., 2014). Furthermore, *in vivo* time-lapse analysis also demonstrates that in the absence of mesoderm progenitors, neural plate cells undergo disrupted dorsal converging movements and embryos develop aberrant neural tube organization (Araya et al., 2014). While this evidence indicates that mesoderm is an essential tissue to regulate orientated displacements of neural plate

cells, the underlying cellular and molecular mechanism by which this tissue interaction is achieved and coordinated during neurulation, remains unknown.

Growing evidence suggests that the extracellular matrix (ECM) has a key role during the development of polarized epithelia and cell migration during tissue organogenesis (O'Brien et al., 2001; Yu et al., 2005; Rozario et al., 2009; Ramussen et al., 2012) reviewed in (Timpl and Brown, 1996; Li et al., 2003; Miner and Yurchenco, 2004; Rozario and Desimone, 2010; De Simone and Mecham, 2013). ECM proteins are largely localized at the basal surface of polarized epithelia, and thus they are ideal molecules to mediate molecular and physical interactions between adjacent tissues during morphogenesis (Bökel and Brown, 2002; Arrington and Yost, 2009) reviewed in (Bonnans et al., 2014). Biochemical and genetic studies have converged to identify the function of key members of the ECM including the basal membrane proteins Laminin (Lam), Fibronectin (Fn) and their cell-surface receptors Integrins (Itg) as critical regulators mediating tissue interaction (Rozario et al., 2009; Morita et al., 2012; Dry et al., 2013). During vertebrate neurulation, Lam, Fn and Collagen proteins become progressively enriched at the deep surface of the neuroepithelium (Martins-Green and Erickson, 1986; Martins-Green, 1988), suggesting that the ECM might have a potential role for neural tube development. In fact, mice mutant for *fn* display defective mesoderm development and aberrant neural tube formation (George et al., 1993). Notably, although these mutants show a short body axis phenotype, they undergo normal gastrulation, indicating the defects only become evident during neurulation stages. Loss of the *lam alpha-5* chain leads to failure of cranial neural tube closure in mice (Miner et al., 1998) and loss of *alpha-3* and *alpha-6 itg* also result in loss of neural tube closure (De Arcangelis et al., 1999) but the mechanism for

these failures is unknown. In zebrafish, Lam and Fn are assembled in between ectoderm and mesoderm just prior to neurulation at about 10 hpf (Latimer and Jessen, 2010; Jessen 2014), and Lam signaling is required for neuroepithelial morphogenesis in brain regions (Gutzman et al., 2008; Buckley et al., 2013; Ivanovitch et al., 2013).

In this work we examine the role of the ECM members, Lam and Fn during early stages of zebrafish neural tube morphogenesis *in vivo*. Using live imaging combined with tissue quantification analysis we show evidence that *lam* and *fn* are required to coordinate the tightly coupled movements of neural plate and mesoderm during dorsal convergence. Our work highlights the role of ECM components in co-ordinating the morphogenetic movements of adjacent tissues.

RESULTS

LamC1 and Fn1 are required for neural tube and mesoderm morphogenesis

We have previously shown that the movements of neural plate and the underlying mesoderm movements are tightly coupled during early stages of zebrafish neurulation. Cells in neural plate and mesoderm move with identical angular speeds, persistence and directionality (Araya et al., 2014). How this coordinated movement of the two tissues is regulated is not certain but one possibility is that the extracellular matrix (ECM) that lies between these tissues could play a significant role in linking their movements.

The neural plate and underlying mesoderm are separated by a basal lamina expressing the two major extracellular matrix proteins Laminin and Fibronectin (Fig. 1A and B) suggesting they could be good candidates to mediate neural-mesoderm interactions. To test this we reduced their function by morpholino (MO) knockdown, using morpholinos previously shown to phenocopy the *lamC1* mutant *sleepy* (Parsons et al., 2002) and the *fn1* mutant *natter* (Trinh and Stainier, 2004). Efficiencies of morpholino knockdowns are shown in Figure 2. Embryos deficient for Fibronectin 1 (*fn1*) alone did not show any obvious neural tube abnormality or defective apico-basal organization, as judged by the expression of the apical protein zonula occludens 1 (ZO-1) at 24 hpf (Fig. 1D). Conversely, downregulation of laminin C1 (*lamC1)* lead to embryos with pronounced neural tubes defects (Fig. 1E) (see also Buckley et al., 2013). Nonetheless, double knockdown embryos displayed even more severely abnormal neural tubes with disorganised apical-basal polarity by 24 hpf (n=18/18 embryos, Fig. 1F). These observations indicate that *fn1* and *lamC1* synergize to control neural morphogenesis.

To determine the onset of the morphogenetic defects following Fn+Lam depletion and to ask whether mesoderm morphogenesis is also affected, we examined mesoderm and brain organization using *in situ* hybridization. We assessed the expression of the neural plate border markers *dlx3* (Akimenko et al., 1994) together with the midbrain hindbrain border marker *pax2.1* (Krauss et al., 2001) and the early mesodermal marker, *papc* (Yamamoto et al., 1998). At the end of gastrulation (up to 12 hpf), *fn1+lamC1* MO embryos were indistinguishable from control MO peers and no defective neural or mesodermal expression was found (Fig. 3A and F). This indicates that either these ECM components are not required for early neural and mesodermal

patterning or that depletion of Lam and Fn by morpholinos is incomplete at this early time point. However, by early neurulation (13 hpf), ECM depleted embryos show some degree of abnormal mesoderm development (Fig. 3D and I) and these changes were amplified later in development. By 14 hpf the neural plate appeared wider and we found the distribution of mesoderm was abnormal in *fn1* and *LamC1* depleted embryos (Fig. 3E and J). Lastly, to confirm the mesoderm disruption in later development, we analyzed the expression of the head mesoderm marker *foxc1a* (Topczewska et al., 2001), and the muscle marker MF-20 (Shimizu et al., 1985) at 24 hpf. We found that *fn1+lamC1* MO embryos have disrupted mesodermal distribution in both head and trunk regions (Fig. 3K and N). Overall these results indicate that the abrogation of ECM function leads to significantly altered morphogenesis of both neural and mesodermal tissues from early neurulation onwards.

ECM is required for close tissue apposition between neuroectoderm and mesoderm

To understand the role that ECM components may have on the relationship between neuroectoderm and mesoderm, we studied embryos by time-lapse microscopy. In wild-type embryos, neural plate and mesoderm lie very close to each other throughout neurulation (Fig. 4A-C) (Araya et al., 2014). In *fn1+lamC1* MO embryos however, we found that small gaps between neural and mesoderm layers were already present at the onset of neurulation (arrowheads in Fig. 4D, 8/8 embryos). These small gaps increase in size during time-lapse capture of neurulation to create an enlarged space between neural tissue and mesoderm (Fig. 4E and F). This space between neural keel and mesoderm appears to be more substantial in *fn1+lamC1* MO embryos embedded

in agarose for live imaging than in non-embedded embryos (not shown), suggesting a physical constraint imposed by embedding in the agarose gel generates additional forces on the embryo that more obviously reveal weaknesses in tissue adhesion. By the end of neurulation (20 hpf), the *fn1+lamC1* MO embryos have failed to generate an organized neural rod with a midline seam where the ventricle should form (Fig. 4F). Analysis of our time-lapse data also reveal that deficiencies of Fn1 and LamC1 lead to a disruption in location and orientation of cell divisions in the neural keel and rod (Fig. 4G), this is similar to the disrupted divisions also seen in MZ*oep* embryos that lack head mesoderm (Araya et al., 2014). These experiments suggest that ECM is required for the close tissue apposition between the neural ectoderm and mesoderm during zebrafish neurulation.

ECM regulates the coupled cell movements between the neural plate and the mesoderm during early neurulation

To determine the consequences of Fn1+LamC1 depletion on the movements of neural plate and mesoderm we analyzed the relative tissue dynamics in *fn1+lamC1* MO embryos by time-lapse imaging (Fig. 5A to D). We have previously shown that cells in neural plate and mesoderm move with identical angular speeds, persistence and directionality during the early stages of neurulation (Fig. 5A and B, Supplementary Movie 1 and quantified in Araya et al., 2014). However analysis of cell movements revealed that the movements of the two layers are independent of each other following ECM depletion (Fig. 5C-I and Supplementary Movie 2). Tracking individual cells in neural plate and mesoderm shows they do not follow similar trajectories. Neural cells make essentially straight tracks as they converge to the

midline but the mesoderm cell tracks are far from straight and not parallel to each other or to the neural cell tracks (Fig. 5F) and they have less consistent directionality plots (Fig. 5G). To quantify this we measured the directional persistence of cell movements and found a significant difference between neural and mesodermal persistence (*fn1+lamC1* MO neural plate cells 0.87 vs *fn1+lamC1* MO mesodermal cells 0.68, $P<0.0001$, Fig. 5H). This contrasts to the wild-type situation where we have previously shown that neural and mesodermal cells move with near identical and parallel tracks (see Fig. 6C in Araya et al. [2014]). Interestingly the Fn+Lam depleted neural cells move with the same persistence as wild-type neural cells (0.87 vs 0.92 respectively, wild-type value taken from Araya et al 2014), but the Fn+Lam depleted mesoderm cells are much less persistent than their wild-type equivalents (0.68 vs 0.93 respectively, wild-type value taken from Araya et al 2014). We also quantified the angular speeds of neural and mesoderm cells in Fn+Lam depleted cells and found these were significantly different (0.072 degrees/min for neural cells compared to 0.051 degrees/min for mesodermal cells, $P<0.0001$, Student's t-test, 180 pairs of cells monitored, 7 embryos, Fig. 5I). The angular speed of both neural and mesodermal cells is reduced compared to wild-type cells (0.072 vs 0.098 degrees/min and 0.051 vs 0.099 degrees/min respectively, wild-type values taken from Araya et al. [2014]).

Together these results demonstrate that cell movements between these tissues are no longer coupled, and that the movements of the mesoderm are more severely disrupted than the movements of the neural plate. Within the *fn1+lamC1* deficient neural plate, neural cells are slower than wild-types but well co-ordinated with each other and able to maintain parallel paths that retain their relative superficial/deep positions as they converge towards the midline (Fig. 5F-I). These experiments reveal that Fn1 and

LamC1 are required to co-ordinate the movements between neural plate and mesoderm during the early stages of zebrafish neurulation.

The mesodermal ECM component Hyaluronan regulates both neural and mesodermal convergence but does not couple their movements

The ECM component Hyaluronan, a glycosaminoglycan, has been shown to be involved in cell migration during organ morphogenesis (Smith et al., 2008) and is required for morphogenesis of both mesoderm and neural tube (Bakkers et al., 2004; Tawk et al., 2007). However since during neurulation stages, Hyaluronan Synthase 2 (*has2*) mRNA is expressed only in mesoderm, how it affects neural plate movements is unclear. One possibility is that the coupling between neural and mesoderm is disrupted following Has2 depletion and this affects neural morphogenesis. To test whether the Has2 phenotype involves an uncoupling of mesoderm and neural movements we analysed their movements by time-lapse microscopy (Fig. 6A and B). Tracking individual cells in Has2 depleted embryos shows that neural and mesodermal cells follow similar essentially straight trajectories as they converge to the midline (Fig. 6C) and they have very similar directionality plots (Fig. 6D). To quantify this we measured the directional persistence of cell movements and found no significant difference between neural and mesodermal persistence (*has2* MO neural plate cells 0.89 vs *has2* MO mesodermal cells 0.87, Fig. 6E). Thus directionality and persistence of movement following Has2 depletion are very similar to those found in wild-type embryos (Araya et al., 2014). We also quantified the angular speeds of neural and mesoderm cells in Has2 depleted embryos and found that although they were not significantly different to one another (Fig. 6F), they were reduced compared

to angular speeds of wild-type cells (0.072 degrees/min for *has2* deficient neural cells compared to 0.098 degrees/min for wild-type neural cells, and 0.073 degrees/min for *has2* deficient mesoderm cells compared to 0.099 degrees/min for wild-type mesodermal cells, wild-type values taken from Araya et al. [2014]). Since Has2 is only expressed in mesoderm and not neural plate these results suggest that the primary consequence of Has2 depletion is a reduction in the speed of the mesoderm, but this leads to a secondary and similar reduction in speed of neural plate movements because these tissues remain coupled by Fn and Lam. This result supports the hypothesis that mesoderm and neural plate are actively coupled, but that Has2 is not responsible for coupling the movements of these two layers.

DISCUSSION

In this work we have shown evidence that depleting the ECM components Laminin and Fibronectin disrupts the tightly coupled movements between neural plate and mesoderm normally observed in wild-type embryos during early neural tube morphogenesis. Furthermore, our observations suggest the ECM rich interface between neural plate and mesoderm is essential to maintain the close apposition between these two layers.

Zebrafish neurulation is initially characterized by the highly organised behaviour of neural plate cells towards the developing dorsal midline (Tawk et al., 2007; Araya et al., 2014). The deposition of ECM proteins from initial stages of neural plate development could suggest that the ECM may serve as a required substrate on which

neural cells move collectively towards the embryonic dorsal midline. Although accumulating evidence has suggested that ECM is required for cell and tissue migration during large-scale tissue rearrangements (Czirók et al., 2004; Zamir et al., 2008; Rozario et al., 2009), whether the ECM is a static or dynamic substratum to achieve tissue migration has not been fully demonstrated (reviewed in Rozario and DeSimone, 2010; De Aleksandrova et al., 2015). In chick embryos for instance, experiments suggest that the ECM moves with a remarkably similar dynamic to the epiblast cells during the initial stages of avian streak formation, demonstrating that the ECM can be a dynamic substrate during global tissue movements (Czirók et al., 2004; Zamir et al., 2008). However, how cells acquire traction during tissue motion in this context is still unclear. Apart for being a physical substrate for neural plate cells migration, ECM on the other hand, may serve as an instructive signal required to polarise or organise cells within the overlying neural plate. This could be particularly critical in those regions where the zebrafish neural plate is a multi-layered structure (such as the prospective hindbrain) and cell position within the superficial/deep axis appears to be tightly regulated during normal neurulation (Araya et al., 2014). With respect to cell behaviour within the neural plate itself, depletion of Fn+Lam has a much milder affect than depletion of mesoderm. We previously showed that neural plate cells in embryos lacking head mesoderm had dramatically disturbed and uncoordinated movements (Araya et al., 2014). One possibility for the mild changes in neural plate movements following Fn+Lam depletion is that the small gaps that appear between neural plate and mesoderm are not sufficient to totally eliminate the critical mesoderm-neural plate interactions that are revealed when head mesoderm is completely missing.

ECM proteins have long been recognized to be required during the development of cell polarity in epithelial morphogenesis both *in vitro* and *in vivo* (Yu et al., 2005; Liu et al., 2007; Martin-Belmonte et al., 2008; Rasmussen et al., 2012; Buckley et al., 2013; Ivanovitch et al., 2013). One possibility therefore is that the defects in neural plate movements and neural tube organisation that follow Fn+Lam depletion are related to aberrant polarity. In the fish, apicobasal polarity or neural cells is not established until late neural rod stages (approximately 19 hpf at the level of the hindbrain, Girdler et al., 2013) and this is about 7 hours after the first defects in neural plate movements are detected in our current study. This suggests the movement defects are unlikely to be related to defects in apicobasal polarity. We show here that neural plate cells move with reduced velocity following Fn+Lam depletion and this could potentially impact on neural tube organisation, but since other aspects of neural plate movements such as persistence and directionality are normal this might suggest a rather limited affect on neural tube morphogenesis through movement defects alone. In fact the movement defects are very unlikely to be the cause of the apicobasal defects seen at 24 hpf because our previous work shows apicobasal organisation develops normally even when the neural plate cells are transplanted to the lateral surface of the embryos yolk mass. In this ectopic location the neural cells aggregate in a totally anomalous way but none the less generate neural cysts with correct apicobasal polarity (Girdler et al 2013). We therefore suggest the defects in apicobasal polarity detected at 24 hpf following Laminin and Fibronectin depletion are most likely a later consequence of the loss of ECM components on apicobasal polarity.

We have yet to investigate the molecular mechanism through which neuroectoderm-mesoderm interactions are mediated by ECM. Several studies have indicated that ECM proteins regulate cell migration and tissue apposition directly by binding Integrin (Itg) receptors (Brower and Jaffe, 1989; Rozario et al., 2009; Morita et al., 2012; Dray et al., 2013). Other studies suggest mechanisms independent integrins might account for the tissue interaction observed during early zebrafish neurulation. In Xenopus, the mechanism of ECM assembly independent of Fn binding activity to Itgs during tissue interaction has been addressed (Rozario et al., 2009). During gastrulation, Fn deposition is required for mesoderm migration under the blastocoel roof (Boucaut and Darribere, 1993; Davidson et al., 2004). By expressing a 70 kD N-terminal fragment of Fn, which genetically blocks Fn assembly, but not the Fn binding to Itg receptors is critical to regulate mesoderm movements (Rozario et al., 2009). Notably, upon over-expression of the 70kD-Fn, mesodermal tissue becomes detached from the BCR and obvious gaps are found between these two layers, suggesting that both tissue-adhesion and cell motility are severely disrupted (Rozario et al., 2009). Interestingly, these results closely resemble our own observations of a loss of tissue adhesion after ECM depletion, suggesting that a similar mechanism that is independent of Itg binding activity could operate in order to promote neuroctoderm-mesoderm interaction. For instance, abrogation of Fn fibrilogenesis leads to an increase in the movement of mesoderm cells during mantle closure stages (Rozario et al., 2009). In the zebrafish, further experiments, combining spatio-temporal genetic tools and live imaging techniques to visualize *in vivo* ECM dynamics will be needed to define the precise contribution of the ECM during neural/mesoderm tissue-interactions.

EXPERIMENTAL PROCEDURES

Ethics Statement

All animal procedures in this study were approved by the College Research Ethics Committee at King's College London (London, UK) and covered by the Home Office Animals (Scientific Procedures) Act 1986 (ASPA) project license.

Zebrafish husbandry

Wild-type zebarfish (*Danio rerio*) were maintained under standard conditions (Westerfield, 1990) at KCL fish facility. Embryos were obtained from timed matings and raised at 28.5°C in egg water or embryo medium (E3). Embryos were staged according to morphologcal criteria and hours post fertilization (hpf) (Kimmel et al., 1994).

Antibody staining

Whole-mount and frozen section antibody staining was performed as recently described (Araya et al., 2014). For primary antibodies, the following primary antibodies were used: mouse-anti-ZO-1 (339111; Zymed Laboratories, South San Francisco, CA, USA) at 1:300; mouse-anti-Laminin1 (L9393; Sigma-Aldrich) at 1:500; rabbit-anti-Fibronectin1 (Sigma-Aldrich) at 1:500; mouse-anti-MF-20 (Developmental Studies Hybridoma Bank, Iowa City, IA, USA) at 1:50, diluted in 2.5% normal goat serum (Sigma-Aldrich). For secondary antibodies, anti-rabbit and

anti-mouse Alexa 488/568/633 (Molecular Probes, Eugene, OR, USA) were used at 1:1000 in 2.5% normal goat serum. Frozen sections were cut every 12 to 14 μm on a Cryo-Star HM 560 MV Micron microtome.

mRNA Synthesis and Morpholino injections

PCS2+ expression vectors carrying (membrane:RFP/GFP or nuclei-h2b-RFP/GFP) were linearized with restriction enzymes for 2 hours at 37°C and precipitated at -20°C overnight in 70% ethanol. DNA was then washed in 70% ethanol and resuspended in nuclease-free water. Sense strand capped mRNA were transcribed using the mMESSAGE SP6 Kit (Ambion) and purified through a column. Resulting RNA concentration will be measured using a spectrophotometer. Antisense morpholinos (MOs) we purchase from Gene Tools, LLC (Corvallis, OR), stored as 4mM stocks at -20°C and diluted as required in sterile water. For ubiquitous knockdown of the protein of interest, MOs were injected at the one cell stage. The following MOs were used in this study: LamC1 MO: (5' TGTGCCTTTTGCTATTGCGACCTC 3') translation-blocking, 3.2 ng (0.4 pmoles)/embryo (Parsons et al., 2002b) and Fn1 MO: (5' TTTTTCACAGGTGCGATTGAACAC 3') translation-blocking, 6ng (0.75 pmoles)/embryo (Trinh and Stainier, 2004).

***In situ* hybridization**

Vectors were linearised and purified as described. *dlx3* (Akimenko et al., 1994), *pax2.1* (Krauss et al., 2001), *papc* (Yamamoto et al., 1998), and *foxc1a* (Topczewska

et al., 2001) anti-sense RNA probes were synthesised using a Dig NTP mix and RNA Polymerase kit (Roche). In situ hybridization was performed as previously described (Topczewska et al., 2001).

Time-Lapse imaging

For live imaging, embryos were mounted in 1.5% low-melting point agarose (A9414, Sigma) in a petri dish filled with egg water or embryo medium (E3), and within an environment chamber at 28.5 C. Time-lapse imaging embryos were imaged at transverse view. For neural plate-mesoderm tracking, embryos we imaged as previously described (Araya et al., 2014). Confocal images were taken 5-10 μm apart using a SP5 Laser Scanning (Leica) a coupled to a 40x long working distance water immersion objective. Z-stacks were recorded every 4-5 minutes and time-lapse imaging started at around 10-11 hpf.

Cell movement quantification

Cell movement analysis was performed as previously described (Araya et al., 2014). Briefly, cropped 4D time-lapse images sequence were assembled in ImageJ software (http://imagej.nih.gov/ij/) and subsequently in QuickTime Pro (Apple, Cupertino, CA, USA). For neural plate-mesoderm cells tracking, the position of cells in their respective germ layer was used as reference. Consecutive frames of the time-lapses was analysed by "Manual Tracking" plugin for ImageJ (http://rsb.info.nih.gov/ij/plugins/track/track.html). Projected tracks, angular velocity and persistence was analysed as previously indicated (Araya et al., 2014). Six to ten

embryos were used in each experimental condition. To test the significance in mean values (standard error of the mean [SEM]), Student's t-test was applied between wild-type ad MO-injected embryos and a probability of 0.05 was accepted as statistically significant.

Statistical Analysis

Microsoft Excel, Prism 5 (Graphpad), and Matlab (R14b; MathWorks, Cambridge, UK) were used for numerical and accompanying statistical analysis. Graphs were created in Prism 5 and Matlab.

ACKNOWLEDGMENTS

We thank all present and past members of the Clarke and Araya labs for critical reading and helpful discussion. We thank Marta Costa for the images in Figure 5A and B. We also thank the KCL Fish Facility staff for help with husbandry. This work was supported by grants from the BBSRC to JDCW and Fondecyt 11110106, Centro Interdisciplinario de Estudios del Sistema Nervioso (CISNe, UACh), and ECOS/Conicyt C13B03 to CA.

Competing interests

The authors declare that they have no competing interests.

Authors' contributions

CA performed and analyzed the majority of the experiments and design experimental strategy. CCF helped to analyze the data of Figures 5 and 6. JDWC oversaw the whole project and wrote the manuscript together with CA. All authors read and approved the final manuscript.

REFERENCES

Aleksandrova A, Rongish BJ, Little CD, Czirók A. 2015. Active cell and ECM movements during development. Methods Mol Biol 1189:123-132.

Akimenko MA, Ekker M, Wegner J, Lin W, Westerfield M. 1994. Combinatorial expression of three zebrafish genes related to distal-less: part of a homebox gene code for the head. J Neurosci 14:3475-3486.

Araya C, Tawk M, Girdler GG, Costa M, Carmona-Fontaine C, Clarke JDW. 2014. Mesoderm is required for coordinated cell movements within zebrafish neural plate in vivo. Neural Dev 9:9.

Arrington CB, Yost HJ. 2009. Extra-embryonic syndecan 2 regulates organ primordial migration and fibrillogenesis throughout the zebrafish embryo. Development 136:3143-3152.

Bakkers J, Kramer C, Pothof J, Quaedvileg NE, Spanik HP, Hammerschmidt M. 2004. Has2 is required upstream of Rac1 to govern dorsal migration of lateral cells during zebrafish gastrulation. Development 131:525-537.

Bonnans C, Chou J, Werb Z. 2014. Remodelling the extracellular matrix in development and disease. Nat Rev Mol Cell Biol 12:786-801.

Bökel C, Brown NH. 2002. Integrins in development: moving on, responding to, and sticking to the extracellular matrix. Dev Cell 3:311-321.

Boucaut JC, Darribere T. 1983. Fibronectin in early amphibian embryos. Migrating mesodermal cells contact fibronectin established prior to gastrulation. Cell Tissue Res 234:135-145.

Brower DL, Jaffe SM. 1989. Requirement for integrins during Drosophila wing development. Nature 342:285-287.

Buckley CE, Ren X, Ward LC, Girdler GC, Araya C, Green MJ, Clark BS, Link BA, Clarke JD. 2013. Mirror-symmetric microtubule assembly and cell interactions drive lumen formation in the zebrafish neural rod. Embo J 32:30-44.

Ciruna B, Jenny A, Lee D, Mlodzik M, Schier AF. 2006. Planar cell polarity signalling couples cell division and morphogenesis during neurulation. Nature 439:220-224.

Clarke J. 2009. Role of polarized cell divisions in zebrafish neural tube formation. Curr Opin Neurobiol 19:134-138.

Czirók A, Rongish BJ, Little CD. 2004. Extracellular matrix dynamics during vertebrate axis formation. Dev Biol 268:111-122.

Davidson LA, Keller R, DeSimone DW. 2004. Assembly and remodeling of the fibrilar fibronectin extracellular matrix during gastrulation and neurulation in Xenopus laevis. Dev Biol 231:888-895.

De Arcangelis A, Mark M, Kreidberg J, Sorokin L, Georges-Labouesse E. 1999. Synergistic activities of alpha3 and alpha6 integrins are required during apical ectodermal ridge formation and organogenesis in the mouse. Development 126:3957-3968.

Dray N, Lawton A, Nandi A, Jülich D, Emonet T, Holley SA. 2013. Cell-Fibronectin Interactions propel vertebrate trunk elongation via tissue mechanics. Curr Biol 23:1335-1341.

George EL, Georges-Labouesse EN, Patel-King RS, Rayburn H, Hynes RO. 1993. Defects in mesoderm, neural tube and vascular development in mouse embryos lacking fibronectin. Development 119:1079-1091.

Girdler GC, Araya C, Ren X, Clarke JD. 2013. Developmental time rather than local environment regulates the schedule of epithelial polarization in the zebrafish neural rod. Neural Dev 8:5.

Gutzman JH, Graeden EG, Lowery LA, Holley HS, Sive H. 2008. Formation of the zebrafish midbrain-hindbrain boundary constriction requires laminin-dependent basal constriction. Mech Dev 125:974-978.

Hong E, Brewster R. 2006. N-cadherin is required for the polarized cell behaviors that drive neurulation in the zebrafish. Development 133:3895-3905.

Ivanovitch K, Cavodeassi F, Wilson SW. 2013. Precocious acquisition of neuroepithelial character in the eye field underlies the onset of eye morphogenesis. Dev Cell 27:293–305.

Jessen JR. 2014. Recent advances in the study of zebrafish extracellular matrix proteins. Dev Biol 14:652-656.

Kimmel CB, Ballard WW, Kimmel SR, Ullmann B, Schilling TF.1995. Stages of embryonic development of the zebrafish. Dev Dyn 203:253–310.

Krauss S, Johansen T, Korzh V, Fjose A. 2001. Expression of the zebrafish paired box gene pax zf-b during early neurogenesis. Development 113:1193-1206.

Latimer A, Jessen JR. 2010. Extracellular matrix assembly and organization during zebrafish gastrulation. Matrix Biol 29:89-96.

Li S, Edgar D, Fässler R, Wadsworth W, Yurchenco PD. 2003. The role of laminin in embryonic cell polarization and tissue organization. Dev Cell 4:613-624.

Liu KD, Datta A, Yu W, Brakeman PR, Jou TS, Matthay MA, Mostov KE. 2007. Rac1 is required for reorientation of polarity and lumen formation through a PI 3-kinase-dependent pathway. Am J Physiol Renal Physiol 293:1633-1640.

Martin-Belmonte F, Yu W, Rodriguez-Fraticelli AE, Ewald AJ, Werb Z, Alonso MA, Mostov KE. 2008. Cell-polarity dynamics controls the mechanism of lumen formation in epithelial morphogenesis. Curr Biol 18:507-513.

Martins-Green M, Erickson CA. 1986. Development of the neural tube basal lamina during neurulation and neural crest cell emigration in the trunk of the mouse embryo. J Embryol Exp Morphol 98:219-236.

Martins-Green M. 1988. Origin of the dorsal surface of the neural tube by progressive delamination of epidermal ectoderm and neuroepithelium: implications for neurulation and neural tube defects. Development 103:687-706.

Miner JH, Cunningham J, Sanes JR. 1998. Roles for laminin in embryogenesis: exencephaly, syndactyly, and placentopathy in mice lacking the laminin alpha5 chain. J Cell Biol 143:1713-1723.

Miner JD, Yurchenco PD. 2004. Laminin functions in tissue morphogenesis. Annu Rev Cell Dev Biol 20:225-284.

Morita H, Kajiura-Kobayashi H, Takagi C, Yamamoto TS, Nonaka S, Ueno N. 2012. Cell movements of the deep layer of non-neural ectoderm underlie complete neural tube closure in Xenopus. Development 139:1417-1426.

O'Brien LE, Jou TS, Pollack AL, Zhang Q, Hansen SH, Yurchenco P, Mostov KE. 2001. Rac1 orientates epithelial apical polarity through effects on basolateral laminin assembly. Nat Cell Biol 9:831-838.

Parsons MJ, Pollard SM, Saude L, Feldman B, Coutinho P, Hirst EM, Stemple DL. 2002. Zebrafish mutants identify an essential role for laminins in notochord formation. Development 129:3137-3146.

Quesada-Hernandez E, Caneparo L, Schneider S, Winkler S, Liebling M, Fraser SE, Heisenberg CP. 2010. Stereotypical cell division orientation controls neural rod midline formation in zebrafish. Curr Biol 20:1966-1972.

Rasmussen JP, Reddy SS, Priess JR. 2012. Laminin is required to orient epithelial polarity in the C. elegans pharynx. Development 139:2050-2060.

Rozario T, Dzamba B, Weber GF, Davidson LA, DeSimone DW. 2009. The physical state of fibronectin matrix differentially regulates morphogenetic movements in vivo. Dev Biol 327:386-398.

Rozario T, DeSimone DW. 2010. The extracellular matrix in developmental and morphogenesis: a dynamic view. Dev Biol 341:126-140.

Shimizu T, Dennis JE, Masaki T, Fischman DA. 1985. Axial arrangement of the myosin rod in vertebrate thick filaments: immunoelectron microscopy with a monoclonal antibody to light meromyosin. J Cell Biol 101:1115-1123.

Smith KA, Chocron S, von der Hardt S, de Pater E, Soufan A, Bussmann J, Schulte-Merker S, Hammerschmidt M, Bakkers J. 2008. Rotation and asymmetric development of the zebrafish heart requires directed migration of cardiac progenitor cells. Dev Cell 14:287-297.

Tawk M, Araya C, Lyons AD, Reugels MR, Girdler CG, Bayley RP, Hyde HD, Tada M, Clarke JDW. 2007. A mirror-symmetric cell division that orchestrates neuroepithelial morphogenesis. Nature 446:779-800.

Timpl R, Brown JC. 1996. Supramolecular assembly of basement membranes. Bioessays 18:123-132.

Topczewska JM, Topczewski J, Shostack A, Kume T, Solnica-Krezel L, Holgan BL. 2001. The winged helix transcription factor Foxc1a is essential for somitogenesis in zebrafish. Genes Dev 15:2483-2493.

Trinh LA, Stainier DY. 2004. Fibronectin regulates epithelial organization during myocardial migration in zebrafish. Dev Cell 6:371-3782.

Yamamoto A, Amacher SL, Kim SH, Geissert D, Kimmel CB, DeRobertis EM. 1998. Zebrafish paraxial protocadherin is a downstream target of spadetail involved in morphogenesis of gastrula mesoderm. Development 125:3389-3397.

Yu W, Datta A, Leory P, O'Brien LE, Mak G, Jou TS, Matlin KS, Mostov KE, Zegers MM. 2005. Beta1-intergrin orients epithelial polarity via Rac1 and laminin. Mol Biol Cell 16:433-445.

Westerfield M: The Zebrafish Book. 2000. A Guide for the Laboratory Use of Zebrafish (Danio rerio). Eugene, OR: University of Oregon Press pp .

Zamir EA, Rongish BJ, Little CD. 2008. The ECM moves during primitive streak formation-computation of ECM versus cellular motion. PLoS Biol 6:e247.

Zigman M, Trinh le A, Fraser SE, Moens CB. 2011. Zebrafish neural tube morphogenesis requires Scribble-dependent oriented cell divisions. Curr Biol 21:79-8.

FIGURE LEGENDS

Figure 1. Depletion of LamC1 and Fn1 lead to severe disruption of neural tube. **A-A'':** Expression of Laminin (Lam) from neural plate to neural tube stages seen in transverse sections. **B-B'':** Expression of Fibronectin (Fn) from neural plate to neural tube stages seen in transverse sections. **C:** Wild-type embryos showing normal expression of the apical marker Zonula Occludends (ZO-1, red) by 24 hpf. **D-E:** Knockdown of either Fn1 or LamC1 results in only minor disruption to ventricle morphology as revealed by ZO-1 expression. **F:** Knockdown of both Fn1 and LamC1 results in more severe disruption to ventricle and neural tube morphology. The normally midline expression domain of ZO1 becomes fragmented and ectopic (yellow arrowheads). Mes, indicates mesoderm, and np indicates neural plate. IV, indicates fourth ventricles in the hindbrain, OV indicates the otic vesicle and hpf, indicates hours post fertilization.

Figure 2. *lamininC1* and *fibronectin1* morpholino efficiencies at neural plate stages. **A-F:** Transverse sections of zebrafish embryos at 11.5 hpf. Laminin immunoreactivity is shown in green in A, B and C. Fibronectin immunoreactivity is shown in red in D, E and F. **A:** Lam reactivity at 11.5 hpf between neural plate and mesoderm. **B:** Reduction of Lam by *lamC1* MO (arrowhead indicate tissue gaps between neural plate and mesoderm). **C:** After *fn1*MO, Lam reactivity shows slightly reduced levels (arrowhead). **D:** Fn reactivity at 12 hpf. **E:** *fn1*MO strongly reduces Fn expression. **F:** After *lamC1*MO, Fn reactivity shows reduced levels (arrowheads). In all pictures np: neural plate and mes: mesoderm.

Figure 3. ECM is required for neural and mesoderm morphogenesis. **A-J:** Analysis of the neural markers *pax2.1* and *dlx3* and the mesoderm marker *papc* (asterisked) show that disrupted tissue organization only arises between 12 and 13hpf in Fn1 and LamC1 deficient embryos. **K-N:** At 24hpf the mesoderm markers *foxc1a* and MF-20 show disrupted distribution of mesoderm in Fn1 and LamC1 deficient embryos. Arrows in N, indicates tissue disruption. Hpf, indicates hours post fertilization.

Figure 4. ECM is required to maintain close tissue apposition of neural tissue and mesoderm. **A-C:** Selected frames from a time-lapse sequence showing close apposition of mesoderm and neural tissue throughout neurulation in wild-type embryo. There is no space apparent between mesoderm and neural tissue. By 20hpf (540 minutes) the neural tube and mesoderm remains closely apposed. **D-F:** Time-lapse sequence from an Fn1/LamC1 deficient embryo showing the presence of gaps between the neural plate and mesoderm from early time point of neurulation (arrowheads). By 20hpf tissue gaps are still present (arrowheads) and neural tube architecture becomes impaired and no clear midline is seen. In A-F, the enveloping layer (evl) has been pseudocolored in blue, neural plate (np) has been pseudocolored in yellow, and the mesoderm (mes) has been pseudocolored in red. Min, indicates minutes and asterisks mean embryo dorsal midline. **G:** Analysis of cell division orientation and location shows the normal midline location of divisions is lost and stereotyped medio-lateral orientation of divisions is disrupted in Fn1/LamC1 deficient embryos.

Figure 5. ECM is required to couple movements of neural plate and mesoderm. **A:** First frame of time-lapse from wild-type (wt) embryo. Image is in transverse plane

and includes left-hand side and midline of neural plate (orientation shown in E). Evl, indicates selected cells in enveloping layer (blue dots), neural plate (yellow dots), and mesoderm (red dots). Arrow indicates midline. Cell nuclei are labeled with H2A-GFP. **B:** Projection of frames 1 to 10 of time-lapse movie from wt embryo, showing the tracks of the selected cells in the EVL, neural plate and mesoderm indicated in A. **C:** First frame of time-lapse from embryo depleted of Laminin and Fibronectin by morpholino injection. Image is in transverse plane and includes left-hand side and midline of neural plate (orientation shown in E). Evl, indicates selected cells in enveloping layer (blue dots), neural plate (yellow dots), and mesoderm (red dots). Arrow indicates midline. Cell nuclei are labeled with H2A-GFP. **D:** Projection of frames 1 to 10 of time-lapse movie from Laminin and Fibronectin depleted embryo, showing the tracks of the EVL, neural plate and mesoderm cells indicated in C. **E:** Diagrams indicating orientation and position of time-lapse movies used for images in A to D and analyses in F to I. Blue layer is enveloping layer (EVL), yellow layer is neural plate (NP) and red layer is mesoderm (MES). **F:** Trajectories of neural (yellow) and mesodermal (red) nuclei in Laminin and Fibronectin depleted embryos. **G-I:** Analyses in cell directionality (G), persistence (H) and angular speed (I), reveals uncoupled behavior of neural plate and mesoderm cells in Fn1/LamC1 morpholno embryos.

Figure 6. Neural plate and mesoderm remain coupled in Has2 deficient embryos. **A:** Frame 1 from a time-lapse sequence of a *has2* deficient embryo. A neural plate (np) nucleus is marked with a yellow dot, a mesodermal (mes) nucleus with a red dot and enveloping layer (evl) nucleus with blue dot. Arrow indicates tissue movements. Midline of neural plate marked with an arrowhead. Orientation and position as for

Fig. 5E. **B:** Frames 1 to 10 of time-lapse superimposed to reveal parallel tracks of neural and mesodermal nuclei. **C:** Trajectories of neural plate (yellow) and mesoderm (red) nuclei on Has2 depleted embryo. **D-F:** Analyses in cell directionality (D), persistence (E) and angular speed (F), reveals movements of neural plate and mesoderm cells remain coupled in Has2 depleted embryos.

SUPPLEMENTARY MATERIAL

Supplementary Movie 1

Neural plate and mesoderm cells move with similar directionality, persistence and speed during early stages of convergence of neural plate. Time-lapse movie at single confocal plane at level of spinal cord in a wild-type, nuclei labeled with H2A-GFP. The left half of the neural plate is shown as indicated in main Figure 5E. Neural plate cell is marked with yellow dot, mesoderm cell with red, and enveloping layer cells with blue. The time between frames is 5 minutes, duration: 45 minutes (from 11 hpf). Arrow indicates embryo midline.

Supplementary Movie 2.

ECM abrogation uncouples the movements between neural plate cells and mesoderm progenitors. Time-lapse movie at single confocal plane at level of the spinal cord in an H2A-GFP injected embryo with have received a previous injection of *fn1+lamC1* MO. GFP labels all nuclei and only the left half of the neural plate is shown as indicated in main Figure 5E. Neural plate cell marked with yellow dot, mesodermal cell with red, and enveloping layer cells with blue. Movements of neural and mesoderm are less coordinated than in wild-type. The time between frames is 5 minutes, duration: 45 minutes (from 11 hpf). Arrow indicates embryo midline.

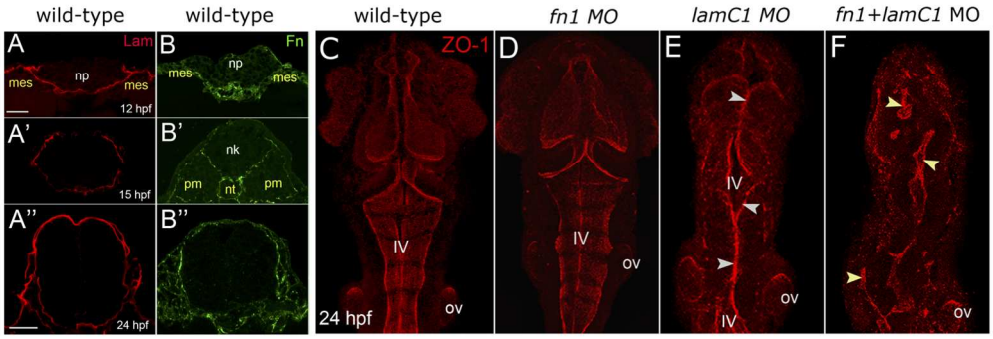

226x81mm (300 x 300 DPI)

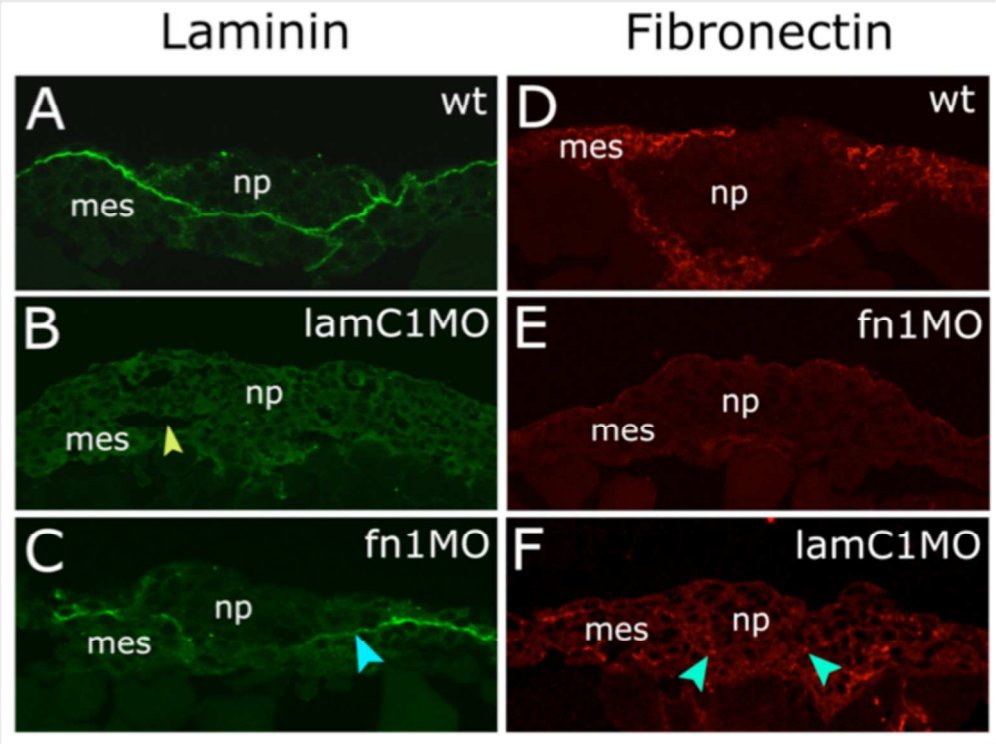

221x166mm (300 x 300 DPI)

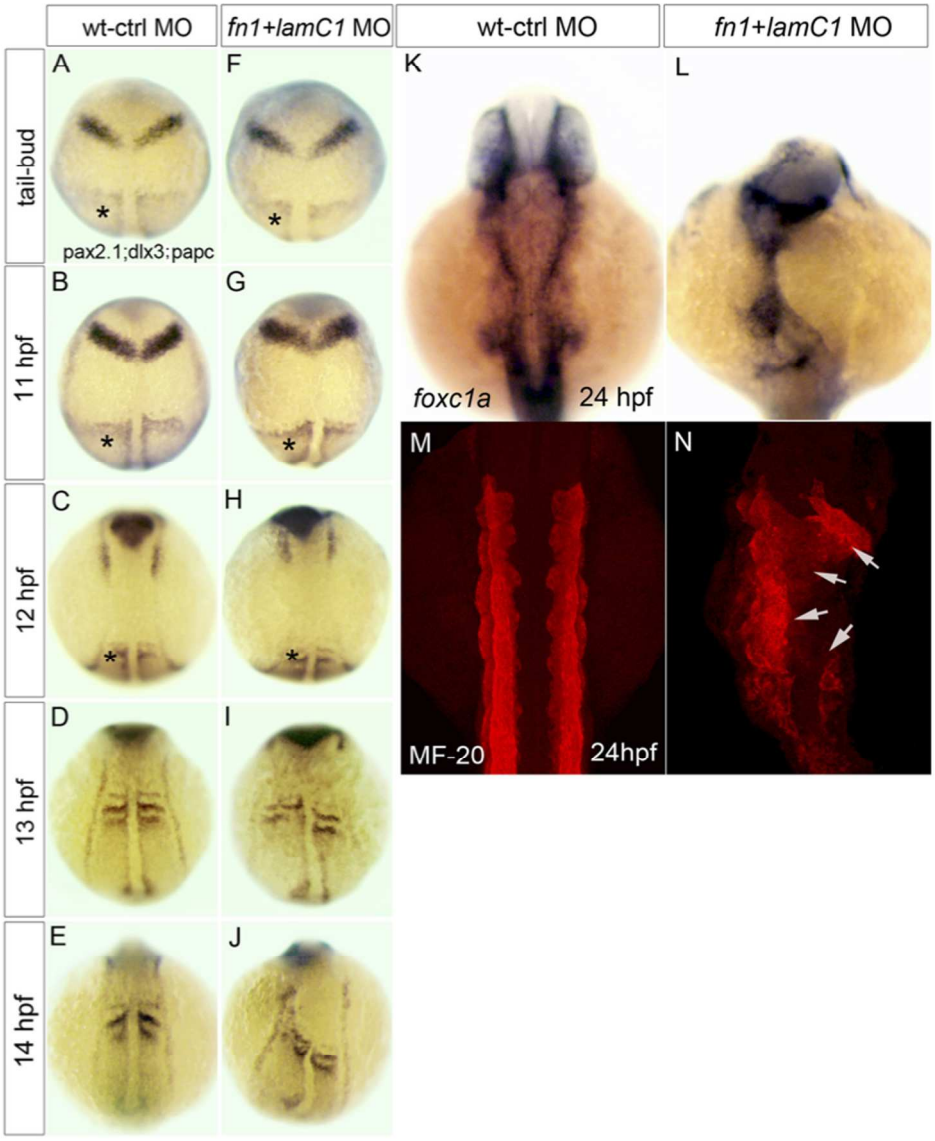

204x242mm (300 x 300 DPI)

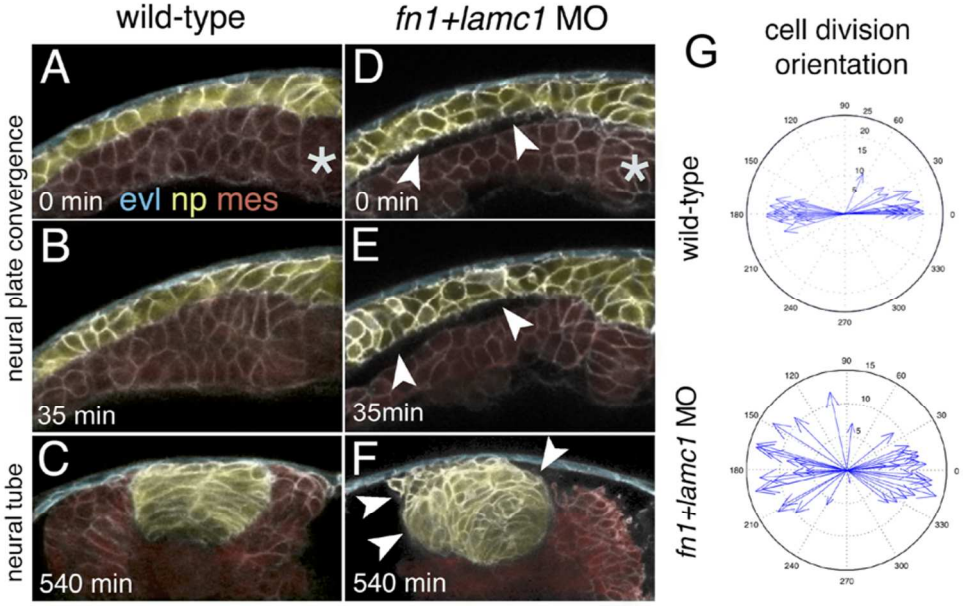

204x131mm (300 x 300 DPI)

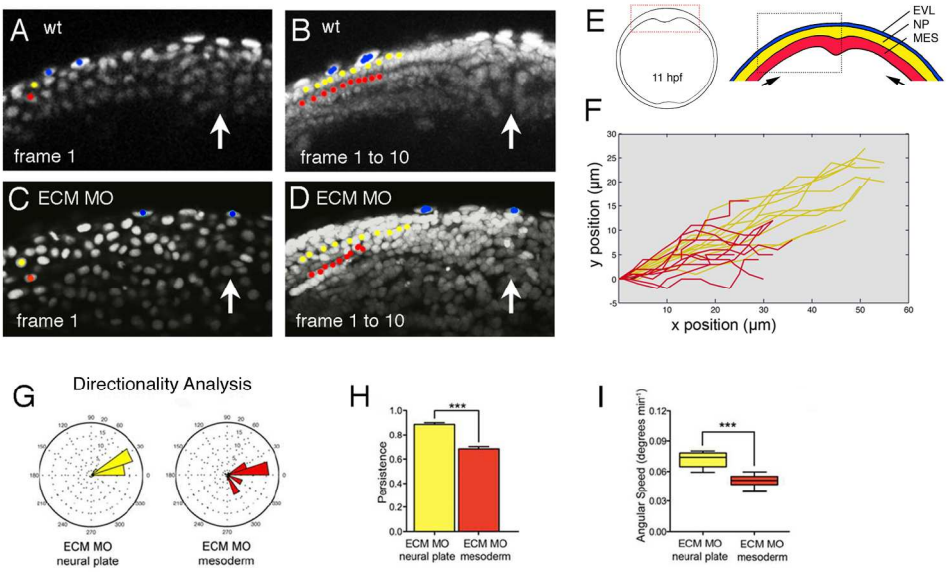

219x133mm (300 x 300 DPI)

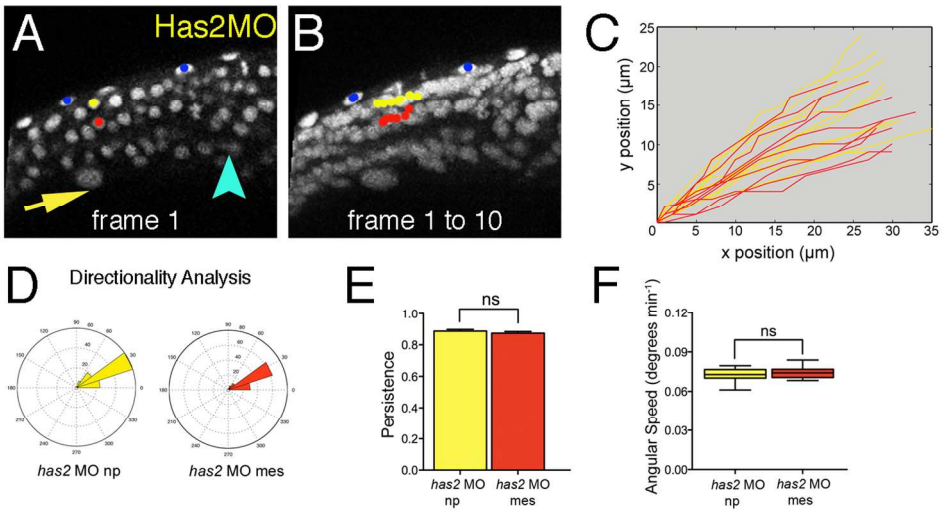

197x104mm (300 x 300 DPI)